Received: 10 February 2019 | Revised: 26 March 2019 | Accepted: 30 March 2019

DOI: 10.1111/iwj.13132

ORIGINAL ARTICLE

IWJ WILEY

Phantom testing of the sensitivity and precision of a sub-epidermal moisture scanner

Lea Peko Cohen | **Amit Gefen**

Department of Biomedical Engineering, Faculty of Engineering, Tel Aviv University, Tel Aviv, Israel

Correspondence
Amit Gefen, The Herbert J. Berman Chair in Vascular Bioengineering, Department of Biomedical Engineering, Faculty of Engineering, Tel Aviv University, Tel Aviv 6997801, Israel.
Email: gefen@tauex.tau.ac.il

Abstract

The majority of pressure ulcers (PUs) including deep tissue injuries (DTIs) are preventable, and even reversible if detected in their early phase. One of the greatest barriers in PU prevention is that clinicians traditionally depended on subjective and qualitative techniques, particularly routine visual skin assessments that would only document existing, macroscopic PUs/DTIs, rather than preventing them or detecting them at their microscopic phase. At the early phase of cell damage, when a forming PU is still microscopic, there is a local increase in extracellular fluid contents within affected tissues, which is called sub-epidermal moisture (SEM). This new understanding has led to an emerging technology, a SEM Scanner (BBI LLC, Bruin Biometrics) that has been designed to effectively examine the health status of tissues, by measuring local changes in the biophysical SEM marker. In the present work, the SEM Scanner was tested under controlled laboratory conditions to experimentally determine its sensitivity and precision in identifying small (1 mL) water content changes in phantoms of the human heel and skull/face, which simulated common PU development scenarios. In both phantom configurations, the locally increased water contents resulted in consistent, statistically significant elevated SEM readings, which confirms that the SEM Scanner is able to detect fluid content changes that are as small as 1 mL. In agreement with a simplified theoretical (mathematical) SEM model, which was also developed here, changes in water contents had a consistent trend of effect on SEM delta values, which increased with each 1 mL increment in intra-tissue-substitute water contents.

KEYWORDS

inflammatory response, oedema, pressure ulcer prevention, prophylaxis

1 | INTRODUCTION

Any form of serious pressure ulcers (PUs, also known as pressure injuries), including a deep tissue injury (DTI), can strongly impact the health status and quality of life of the affected individual.[1] Approximately 60 000 patients die each year because of infections and complications from PUs.[2–4] These wounds also impose a heavy financial burden with average treatment costs exceeding 26.8-billion dollars annually in the United States alone.[5–10] Considering the above, the current global consensus is that PU prevention (PUP) is where most health care resources need to be invested in, particularly because the majority of PUs are preventable and even reversible if detected in their early phase of development.[11,12]

One of the greatest barriers in PUP is that clinicians traditionally depended on routine visual skin assessments (VSAs),

which are an integral part of nearly all risk assessment and at-risk patient management protocols.[1,13,14] The subjective, qualitative, and intra-rater-variable VSAs[15] are subject to failure when used to detect category-1 PUs and suspected DTIs, especially in patients with dark skin colour or if the care provider is relatively inexperienced.[15–19] Moreover, even at a best-case scenario, VSAs will only successfully document the present condition of an existing PU or tissue damage (as observed at the skin surface), rather than preventing these. In addition to VSAs, ultrasound (US) technology is gaining popularity in PUP work, although mostly as a research technique at this time. The application of US to PUP has focused mainly on identifying structural changes in tissues, which are visible to the radiologist as hypoechoic lesions or discontinuities in tissue layers, and may point to macroscopic subdermal tissue damage.[15,20–25] However, US (much like VSAs) is unable to detect damage while it is still microscopic and limited to small groups of cells, at which time the damage could still be completely reversible and repairable by the body systems.[15,26] Moreover, US has other disadvantages that are remarkably similar to those of VSAs, namely, US requires expertise and substantial experience in order to make a meaningful diagnosis, it is subjective (eg, two US experts may interpret the same US scan differently), and is qualitative in nature.

Over the two recent decades, PU research has made immense progress in understanding the aetiology of PUs and the deep tissue damage spiral in particular.[1,27] There is a new understanding that at the early phase of damage, when the forming PU is still microscopic and limited to a small number of cells (and is most likely reversible), there is a mild, local increase in extracellular fluid contents within the affected tissues because of the inflammatory process, which is triggered by the death of the first cells.[15,28–30] This local rise in tissue fluid contents is caused by the increased permeability of the vascular walls near the cell death site, which allows immune system cells to migrate from the blood circulation to the forming damage site. The biophysical measure of the aforementioned localised oedema is called subepidermal moisture (SEM), which has been investigated in many clinical studies that altogether established the association of SEM changes with the early-stage, not necessarily visible PUs.[18,19,31–35]

This scientific progress has led to an emerging technology that has been designed to effectively examine the health status of tissues under the skin surface in at-risk individuals by monitoring and detecting local SEM changes. The medical device, called the SEM Scanner (BBI LLC, Bruin Biometrics, Los Angeles, California), is a hand-held device that has been approved by the US Food & Drug Administration (FDA) for examination of the sacral and heel areas as an adjunct to clinical assessment. The SEM Scanner has been evaluated and proved to be clinically effective in both prevention and early-detection of PUs and DTIs through measurements of spatial and temporal variations of SEM readings at an anatomical site.[15,18–20,29,32,33,35–39] Multiple studies have specifically demonstrated that the SEM Scanner is able to detect DTIs before they are visible to the unaided eye, and that abnormal SEM measurements precede abnormal VSA outcomes by up to 10 days.[15,32,33,36,37] The SEM Scanner has also been compared with US in a clinical study, where SEM readings were abnormal 3 days before the appearance of a hypoechoic lesion indicating a forming DTI in the US examination.[15]

Key Messages

- we describe laboratory tests for experimentally determining the sensitivity and precision of a subepidermal moisture (SEM) Scanner in identifying small (1 mL) water content changes in human phantoms of the heel and skull/face, which simulated common pressure ulcer development scenarios
- in both phantom configurations, the locally increased water contents resulted in consistent, statistically significant elevated device readings, which confirm that the SEM Scanner is able to detect fluid content changes of 1 mL
- accordingly, this work demonstrates that the SEM Scanner is a sensitive and robust device for examination of invisible damage signs caused by sustained tissue deformations

In the present work, the SEM Scanner was used for the first time in a laboratory study to experimentally detect water content changes in two artificial substitutes (phantoms) of a human anatomy: (a) The posterior heel as an example for a PU forming because of the sustained bodyweight forces (weight of the foot) and associated heel tissue deformations, and (b) The left cheek and the chin as examples for a PU forming because of sustained tissue deformations caused by a medical device, that is, a continuous positive airway pressure (CPAP) mask in this case. It is noteworthy that in the context of the heel phantom studies, the posterior aspect of the heel is the second most common anatomical site for PU development associated with chronic supine bedrest.[40–47] Likewise, in the context of medical device-related PUs, facial tissues are commonly injured by CPAP masks.[48–56]

Using the above laboratory phantoms, our goal was to experimentally determine whether there is a statistically significant difference between SEM readings associated with certain water contents at the affected tissue site (also termed the "target site"), vs different water contents at another, adjacent "reference site." Hence, by means of the phantoms

described above, we evaluated the sensitivity and precision of the SEM Scanner and have characterised its mode of operation in a well-controlled laboratory setting.

1.1 | Theoretical background of biocapacitance measurements

The SEM Scanner is a hand-held device that measures the biocapacitance of tissues at a depth of several millimetres under the skin. Unlike the various medical devices, which measure the bioimpedance of tissues by applying a fixed frequency signal and then measuring the voltage difference at the receiving electrode, the SEM Scanner does not excite the alternating current signal through the tissue itself. Accordingly, SEM Scanner measurements do not depend on the resistivity and conductivity of the examined tissues. Briefly, when pressed against an area on the skin with adequate pressure, the SEM Scanner measures the sub-epidermal biocapacitance by applying a low-frequency signal through the external capacitor; the signal response is affected only by the dielectric characteristics and the amount of fluids in the examined tissue, which is then compared with the charge of the internal reference capacitor. The measure of biocapacitance is then translated into a calibrated SEM (dimensionless) value. The penetration depth of measurements depends on the size of the probe of the device.

The simplified SEM biocapacitance model is shown in Figure 1A. It consists of two parallel conducting plates that are separated by a distance d. In this simplified model, the SEM electrodes measure the biocapacitance of soft tissues with a total thickness d that contain a mass of fluid t representing the SEM contained in the examined tissues. The biocapacitance C (in Farads) is defined by:

$$C = \frac{Q}{|\Delta V|} \tag{1}$$

where Q is the electrical charge and ΔV is the potential difference between the plates of the electrode. To find the biocapacitance of the tissues C, we first calculate the potential difference between the conductive plates ΔV. The electric field E_d between the plates in this simplified configuration (in Volts/m) is given by:

$$E_d = \frac{E_0}{\kappa_e} = \frac{Q}{\varepsilon_0 \kappa_e A} \tag{2}$$

where E_0 is the electric field without a dielectric material, ε_0 is the absolute permittivity in a vacuum and κ_e is a dielectric constant of water.

$$\Delta V = -\int_{+}^{-} E dl = -E_0(d-t) - E_d t = -\frac{Q}{\varepsilon_0 A}(d-t)$$

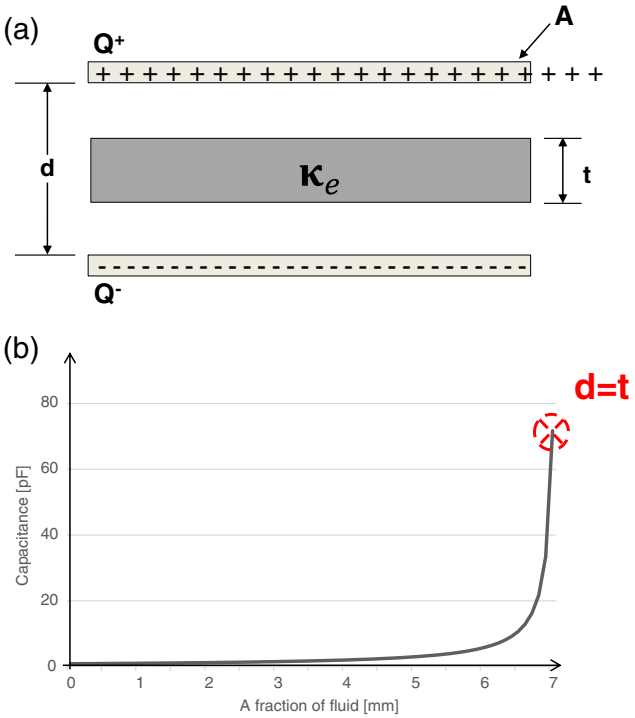

FIGURE 1 A, The simplified sub-epidermal moisture (SEM) biocapacitance model consisting of two parallel conducting plates that are separated by a distance d. The SEM electrodes measure the biocapacitance of soft tissues with simplified total thickness d that contain a fraction of fluid; the fluid mass is represented as a dielectric material with thickness t that is contained between the plates. B, The biocapacitance values were calculated for increasing fluid contents t within the tissue. The area of the conductive plates was taken as 7 cm^2 and the examined total soft tissue thickness d was 0.7 cm. Q = the electrical charge on the plates, A = area of the conducting plates, d = the distance between the plates (total examined soft tissue thickness), t = the fluid contents within the tissue (the fluid fraction is t/d), and κ_e = the dielectric constant of water

$$-\frac{Q}{\varepsilon_0 \kappa_e A} t = -\frac{Q}{\varepsilon_0 A}\left[d - t\left(1 - \frac{1}{\kappa_e}\right)\right] \tag{3}$$

The potential difference ΔV can now be formulated by integrating the local electric field E along a straight line from the top to the bottom plate:

Substituting the above result for ΔV (Equation 3) in Equation (1) results:

$$C = \frac{\varepsilon_0 A}{d - t\left(1 - \frac{1}{\kappa_e}\right)} \tag{4}$$

The formulation in Equation (4) demonstrates that the biocapacitance C depends only on the geometry of the plates (electrodes) and fluid contents t. The biocapacitance increases linearly with the area of the plates because for a given potential difference, a larger plate can hold more electrical charge. Furthermore, the biocapacitance is inversely

proportional to the thickness of the examined soft tissue. Hence, this theoretical modelling (which is a first-order approximation of the physical principles of operation of the SEM Scanner) predicts that SEM measurements would result in lower biocapacitance readings at thicker soft tissue regions (where d is larger) for the same mass of contained fluids represented by t. In order to visualise the predictions of this simplified model, biocapacitance values were calculated for an increasing fluid contents in tissues that are 0.7 cm thick, which are examined by conductive plates (electrodes) with a size of 7 cm^2 (Figure 1B). It is shown that the biocapacitance measure C is highly non-linear, rises rapidly after exceeding the critical fluid content level (the inflection point or "knee" in the curve) and approaches the biocapacitance of water as fluids t fill the space d:

$$C \to \frac{\varepsilon_0 \kappa_e A}{d} = \kappa_e C_0 \tag{5}$$

where the constant C_o represents the capacitance for vacuum between the plates.

2 | METHODS

In the clinical practice of SEM Scanner-aided PUP, the SEM delta (Δ) is a biophysical marker associated with localised oedema (ie, elevated tissue fluid contents), which forms early in the damage spiral, with the onset of the inflammatory phase. The delta is the difference between two SEM readings, one taken at the anatomical site that is at the highest risk or where there is a suspected evolving injury and the other is from a presumably unaffected site in the vicinity. The greater the SEM delta is, the higher is the risk of developing a visible PU at the examined anatomical location.

2.1 | Experimental protocol for studying the posterior heel

First, we have three-dimensionally (3D) printed a phantom of the skeleton of the left heel, which was created from segmentation of the calcaneus, talus, and navicular bones based on the Visible Human (male) database (National Library of Medicine, United States, https://www.nlm.nih.gov/research/visible/visible_human.html) (Figure 2A, left frame). For a soft tissue substitute, we used 0.7 cm-thick baby diaper cuts (Life Babies, Superpharm Co., Israel), which we have attached to the posterior aspect of the calcaneus. For this purpose, the diapers were cut to square-shape, 4.5 cm-wide samples. The aforementioned thickness of these diaper samples is representative of soft tissue thickness at the posterior heel of healthy subjects, as documented in our previous magnetic resonance imaging work.[57]

Next, two diaper samples were attached to the calcaneus bone of the heel model: A "reference" sample was placed at the lateral left aspect of the calcaneus, and a "test" sample was attached at the posterior calcaneal aspect, which is the most common site for heel ulcer (HU) development (Figure 2A, right frame). Next, we injected known water contents to the samples. The reference sample was repeatedly loaded with 1 mL of water, whereas the test sample was loaded with increasingly varying water contents of 2, 3, and 4 mL to simulate a potential development of localised oedema at the posterior heel aspect as in early HU formation. We then used a SEM Scanner to determine the delta of SEM readings between the test and reference locations, and readings were always taken from the reference location first (Figure 2B). The delta of SEM readings was calculated per each experimental condition, that is, for water contents of 2, 3, and 4 mL at the test location.

2.2 | Experimental protocol for studying the skull/face phantom

Similar to the above heel phantom work, the left cheek and the chin have been studied using a skull phantom made of rigid plastic (Figure 3A, left frame), onto which test and reference diaper specimens have been attached to represent soft tissues. For this purpose, 0.7 cm thick baby diapers were cut to 5.5 cm wide square-shape samples, which were then attached together in pairs (to make the soft tissue substitutes 1.4 cm thick) (Figure 3A, right frame) and mounted at the left cheek and the chin locations of the skull model. The aforementioned total thickness of the diaper sample pairs is representative of facial soft tissue thickness at the cheeks and chin of healthy subjects, as measured in an anatomically realistic 3D adult head model built using the visible human (male) project image database[58] in a previous research study in our group.[59] Next, two sample pairs were attached to the left cheek of the skull/face phantom model. A test sample pair was mounted at the anterior aspect of the maxilla bone at the left cheek, which is a common facial site for CPAP-use-related PUs. The respective reference sample pair was placed at the lateral left aspect of the zygomatic bone (Figure 3B). Similarly, two sample pairs were attached at the chin. A test sample pair was attached to the anterior jawbone and the corresponding reference sample pair was placed at the lateral left aspect of the mandible (Figure 3C). In each sample pair, only the top layer was wetted with known water contents. The reference sample has been repeatedly loaded with 1 mL of water, whereas the test sample was loaded with increasingly varying water contents of 2-4 mL (at 1 mL intervals). The SEM measurement protocol for determining

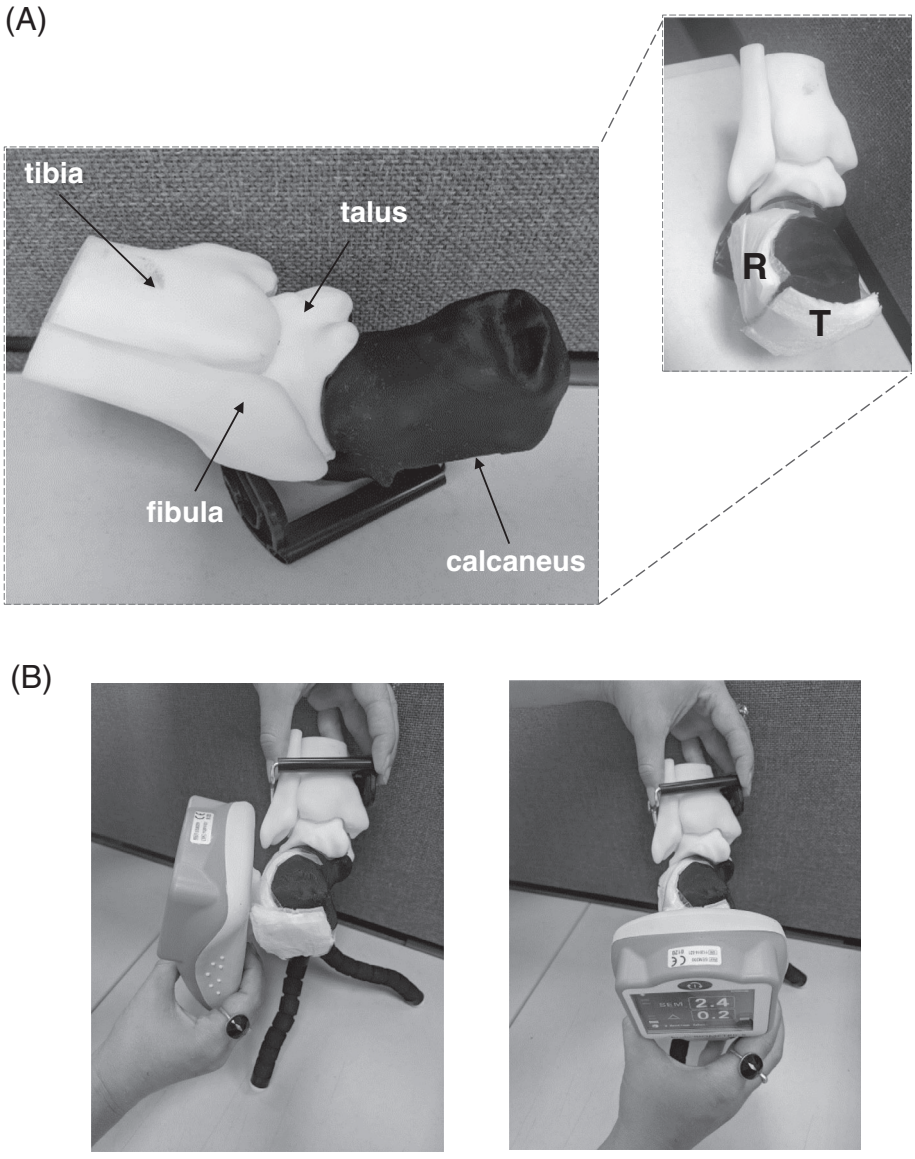

FIGURE 2 The heel phantom model: A, A three-dimensionally (3D) printed heel skeleton model (left frame). For the heel sub-epidermal moisture (SEM) measurements, a reference diaper sample was placed at the lateral left aspect of the calcaneus and a test sample was attached at the posterior calcaneal aspect (right frame). B, Acquisition of SEM readings at the reference (left frame) and test (right frame) locations. T = test and R = reference samples

the delta of SEM readings between the test and reference locations in this skull/face phantom was the same as for the heel phantom model.

2.3 | Data collection and statistical analysis

The following data collection procedure has been conducted separately for each phantom configuration (heel, skull). We have repeated each delta measurement 10 times, per water content level at the test location (2, 3, and 4 mL) and each SEM reading was taken 5 times 1 minute and then 2 minutes after wetting the samples. The delta values were calculated separately for the 1 and 2 minutes time points. Because measurements were indistinguishable between these two time points, they were pooled for each water content level. We calculated descriptive statistics (means and SDs) for the SEM deltas, per each water content at the test location. Finally, for each phantom configuration, we conducted a one-way analysis of variance for the factor of water contents in the test sample, to determine whether the delta differed significantly across the different water content conditions at the test site. We considered *P* values of less than .05 statistically significant.

3 | RESULTS

Mean delta values and respective SDs for the two phantom configurations, the heel and skull/face, are provided in Table 1. For both phantom configurations, the SEM Scanner was shown to be able to be sensitive enough to detect the variation in water contents, and the increase in volume of water has demonstrated a corresponding consistent trend of increasing deltas with each increase in the water content (Table 1). For the heel phantom, increasing the test—

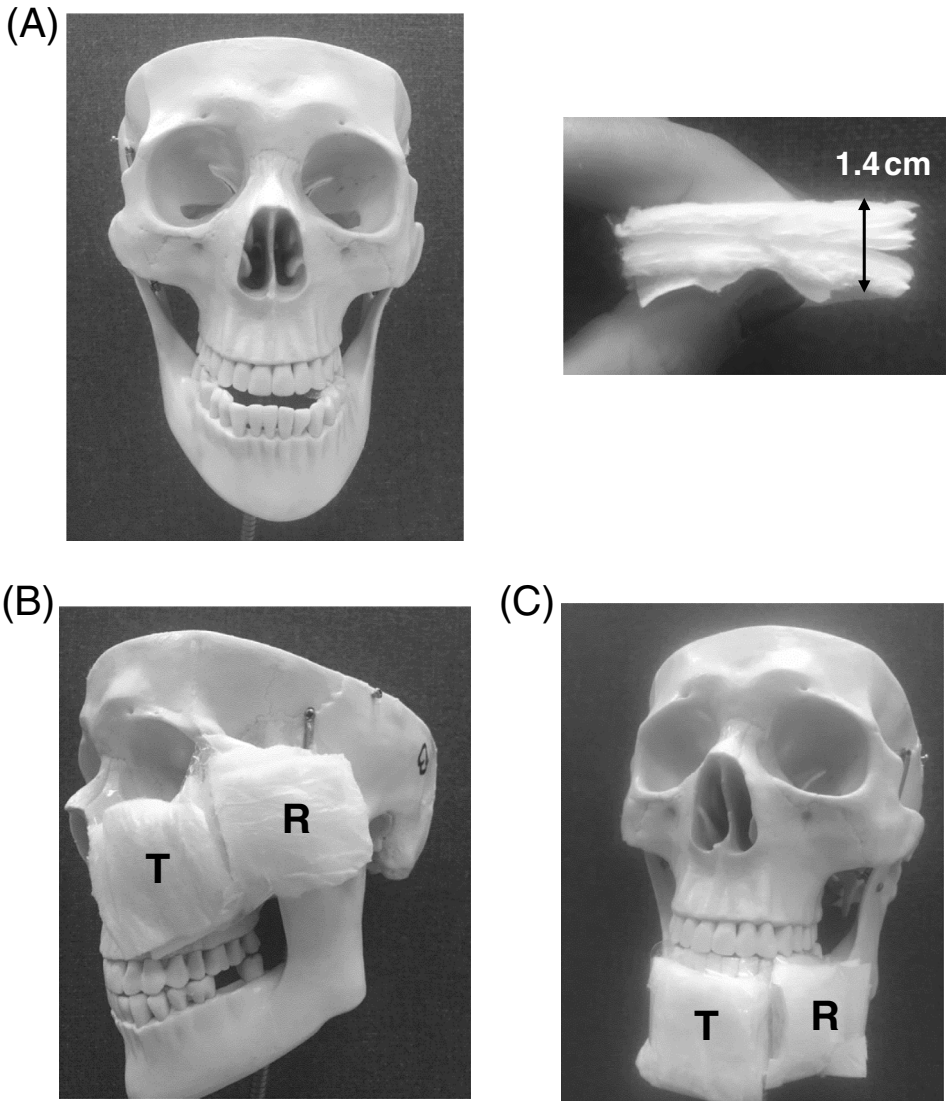

FIGURE 3 The skull/face phantom model: A, A front view of the skull (left frame) with a diaper sample pair as a soft tissue substitute (right frame). B, For the left cheek sub-epidermal moisture (SEM) measurements, a test diaper sample pair was attached at the anterior aspect of the maxilla bone and a reference diaper sample pair was placed at the lateral left aspect of the zygomatic bone. C, For the chin SEM measurements, a test sample pair was attached to the anterior jawbone and a reference sample pair was placed at the lateral left aspect of the mandible. T = test and R = reference samples

reference difference in water contents by 2 and 3 mL resulted in a statistically significant increase in SEM readings by 100% and 167% with respect to the 1 mL difference case (Table 1 and Figure 4A, $P < .00001$ for both conditions). Likewise, for the skull phantom, increasing the test—reference difference in water contents by 2 and 3 mL resulted in a statistically significant increase in SEM readings, by 50% and 100% with respect to the 1 mL difference case (Table 1 and Figure 4B and C, $P < .0003$ for both conditions). Accordingly, we demonstrated that as the theory of the simplified SEM biocapacitance model (Figure 1A) predicts, the biocapacitance measure C and the associated SEM values rise for increasing fluid contents within the affected (simulated) tissue sites. Furthermore, our present empirical findings also confirmed the first-order approximation of the physical principles of the SEM model, which predicts lower SEM values at thicker soft tissues regions (where d is greater) for the same mass of contained fluids (t) (Equation (4)).

TABLE 1 Sub-epidermal moisture delta readings for increasing water content differences between a test and reference site for the heel and skull/face phantoms

Water content difference between test and reference site (mL)	Δ for heel	Δ for the left cheek	Δ for the chin
2 − 1 = 1	0.3 ± 0.07	0.2 ± 0.06	0.2 ± 0.09
3 − 1 = 2	0.6 ± 0.11	0.3 ± 0.06	0.3 ± 0.05
4 − 1 = 3	0.8 ± 0.18	0.4 ± 0.09	0.4 ± 0.07

4 | DISCUSSION

In the present work, we aimed to evaluate the sensitivity and precision of the SEM Scanner in detecting different water contents in target tissue sites vs nearby reference sites (SEM delta) at simulated anatomical locations susceptible to PUs. For this purpose, we developed and used two laboratory

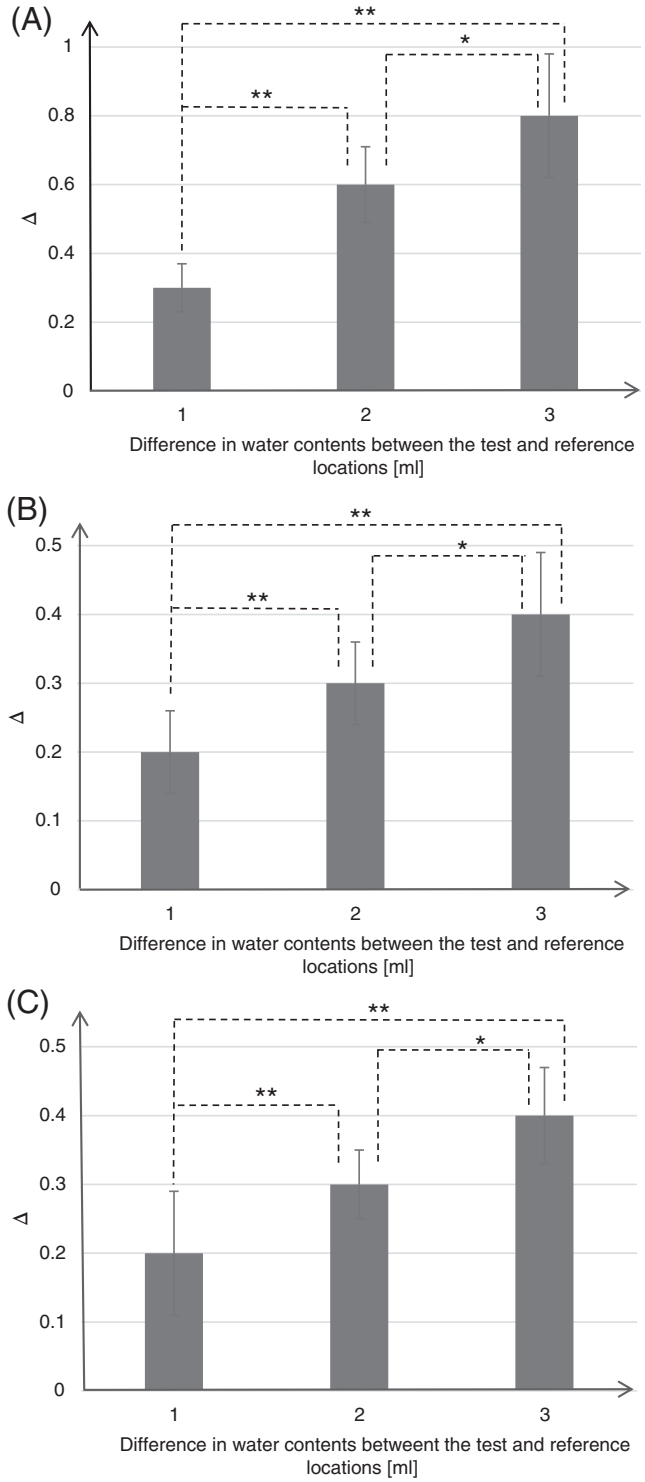

FIGURE 4 Means and SDs of sub-epidermal moisture (SEM) delta values, calculated as a difference between SEM readings at the reference sample (loaded with 1 mL water) and test sample (loaded with 2, 3 or 4 mL water) for the heel phantom (A) and for the skull/face phantom at the left cheek (B) and the chin (C). The statistically significant differences marked on the bar graphs were $*P < .003$ and $**P < .00001$ for the heel phantom (A), and $*P < .02$ and $**P < .0003$ for the skull/face phantom (B, C)

phantom models of a human anatomy: (a) the posterior heel as an example for PUs forming because of sustained bodyweight forces, and (b) the left cheek and the chin as examples for facial anatomical sites at risk for PU development because of sustained tissue deformations caused by a CPAP ventilation mask. Our goal was to test whether the SEM Scanner is sensitive and able to detect small variations in water contents at the affected vs reference tissue sites in our simulated micro-oedema cases.

In both phantom configurations, we demonstrated experimentally that locally increased water contents at the aforementioned simulated body sites resulted in elevated SEM delta readings, which confirms that the SEM Scanner is able to detect fluid content changes that are as small as 1 mL. This establishes validity and sensitivity of the SEM Scanner under well-controlled laboratory conditions, which is reported here for the first time in the literature. Specifically, we found statistically significant differences in SEM delta readings acquired for water content differences of 1, 2, or 3 mL between the affected and (adjacent) reference sites across all anatomical locations in both types of phantoms (Figure 4). Accordingly, we demonstrate here that the biocapacitance measure C and the associated SEM readings rise for increasing fluid contents within the affected (simulated) tissue sites, as theory (Equation 4) has predicted. Bearing in mind that a forming PU involves build-up of oedema because of immune system response to cell death, our present findings are consistent with previously published clinical research that repeatedly identified strong correlations between elevated SEM delta readings and the risk of developing visible PUs (eg, at the heels or sacrum).[15,20,26,29,32,33,35–39]

Furthermore, our present empirical findings also confirmed the theoretical SEM biocapacitance model (Figure 1A), demonstrating lower SEM readings at thicker soft tissues regions (where d is greater) for the same mass of contained fluids (t) (Equation (4)). In the current study, we used 0.7 cm-thick diaper cuts as a soft tissue substitute in the heel phantom (d_h) and 1.4 cm-thick soft tissue substitute in the skull/face model (d_s). Considering that the thickness of the soft tissue substitute in the heel phantom was half that of the skull phantom ($d_h = d_s/2$), and that the reference and test samples have been repeatedly loaded with the same mass of fluid (t) in both phantom types, it can be expected from theory that the SEM measurements would result in greater SEM readings in the heel configuration (Equation (4)). Indeed, our data show that the SEM readings collected from the heel phantom were 1.5-fold to 2-fold greater than for the skull phantom (for corresponding fluid masses). This further confirms our theoretical predictions that the biocapacitance readings should be approximately

inversely proportional to the thickness of soft tissues at the examined site (Equation (4)).

Overall, we found that the SEM Scanner is sensitive enough to detect slight (1 mL) changes in sub-epidermal water contents, which confirms its role in the early detection of PUs and explains its clinical efficacy that has been demonstrated in multiple different clinical trials.[15,20,29,32,33,35–39] The SEM Scanner is already an established clinical technology for early detection of PUs, and as stated above, it has recently been approved by FDA for clinical use in the United States. Nevertheless, it is still necessary to understand its underlying physical principles and sensitivity parameters for achieving additional progress in technology development and protocols of implementation. Unlike US and VSA, which focus on macroscopic pathoanatomical changes, the SEM Scanner is able to detect the micro-changes in fluid contents, which are associated with the earliest onset of cell damage, by monitoring the tissue bio-capacitance.[26,34,60,61] The slight changes in water contents that are shown here to be detectable by the SEM Scanner may precede the appearance of a hypoechoic lesion in an US examination[15] and the visible VSA findings at the skin surface several days afterward.[15,32,33,35–39] At the earliest phase of PU formation, when there is only microscopic cell and tissue damage, typically under intact skin, there is a small increase in extracellular fluid contents because of the increased capillary permeability, which enables infiltration of the immune system cells to the damaged area.[15,20,29,30] By monitoring these aforementioned microscopic water content changes that cannot be detected visually or timely by other modalities, the SEM Scanner provides caregivers the ability to determine a risk or early-detect a forming PU and then intervene timely to stop and reverse the micro-damage.

The present work clearly shows that the SEM Scanner is a sensitive tool for examination of invisible signs of physiological damage caused by sustained tissue deformations. Nevertheless, as always, there are inherent limitations related to the experimental work. For example, we did not use heat-generating phantoms to mimic body or tissue temperature, or simulated sweating, muscle contractions, and episodes of skin wetness or any other physiological tissue behaviour not directly related to the sub-epidermal water contents (but with a potential influence on water contents in tissues). With that being said, perhaps the most important advantage of physical phantoms is their ability to isolate a specific phenomenon of interest and eliminate any other interference or biasing factors that contribute to inter-subjects and intra-subject biological variability.

Despite the evident clinical benefit of the SEM Scanner, modes of action of the device needed explanation through laboratory bioengineering work, and the present study served that purpose. In conclusion, the SEM Scanner was shown to be sensitive enough to detect as small as 1 mL variations in water contents within simulated tissues in physical phantoms representing human anatomy and clinical scenarios. In agreement with the theory of biocapacitance, which has been formulated here, changes in water contents had a consistent trend of effect on SEM delta measurements, which increased with each 1 mL increment in intra-tissue-substitute water contents. Accordingly, this work demonstrates for the first time that the SEM Scanner is sensitive and robust under controlled laboratory conditions simulating clinical use, which complements and supports the body of published clinical evidence.[15,20,26,29,32,33,35–39] The SEM Scanner is a technological breakthrough in PUP, which is able to detect physiologically and clinically relevant information concerning tissue health status in at-risk individuals. As an adjunct to standard care, the SEM Scanner has a pivotal and pioneering role in PUP.

ACKNOWLEDGEMENTS

Ms Hadar Shaulian, doctoral student (co-advised by Prof A.G.), Faculty of Mechanical Engineering, Technion—Israel Institute of Technology, for the 3D printing of the heel bones and assembling the printed heel skeleton.

DISCLOSURE

Dr A.G. acts as a scientific advisor to multiple companies in the field of pressure ulcer/injury prevention, including Bruin Biometrics LLC, Los Angeles, California) whose SEM Scanner technology is evaluated in this article. This had no influence on the study design or conclusions from the analysis of laboratory test data that are presented here.

ORCID

Amit Gefen https://orcid.org/0000-0002-0223-7218

REFERENCES

1. European Pressure Ulcer Advisory Panel (EPUAP) and National Pressure Ulcer Advisory Panel (NPUAP) International Guidelines (2014). Internationalguideline Web site. www.internationalguideline.com. Accessed April 6, 2019.
2. VanGilder C, Amlung S, Harrison P, Meyer S. Results of the 2008-2009 International Pressure Ulcer Prevalence Survey and a 3-year, acute care, unit-specific analysis. *Ostomy Wound Manage*. 2009;55(11):39-45.
3. Vanderwee K, Clark M, Dealey C, Gunningberg L, Defloor T. Pressure ulcer prevalence in Europe: a pilot study. *J Eval Clin Pract*. 2007;13(2):227-235.

4. Pressure ulcers in America: prevalence, incidence, and implications for the future. An executive summary of the National Pressure Ulcer Advisory Panel monograph. *Adv Skin Wound Care*. 2001;14(4):208-215.
5. Gefen A. The biomechanics of sitting-acquired pressure ulcers in patients with spinal cord injury or lesions. *Int Wound J*. 2007;4: 222-231.
6. Miller H, Delozier J. *Cost Implications of the Pressure Ulcer Treatment Guideline*. Columbia, MD: Center for Health Policy Studies. (Contract No. 282-91-0070. Sponsored by the Agency for Health Care Policy and Research); 1994.
7. Duncan KD. Preventing pressure ulcers: the goal is zero. *Jt Comm J Qual Patient Saf*. 2007;33:605-610.
8. Padula WV, Delarmente BA. The national cost of hospital-acquired pressure injuries in the United States. *Int Wound J*. 2019. https://doi.org/10.1111/iwj.13071.
9. Lyder CH, Ayello EA. Pressure ulcers: a patient safety issue. In: Hughes RG, ed. *Patient Safety and Quality: An Evidence Based Handbook for Nurses*. Rockville, MD: Agency for Healthcare Research and Quality (US); 2008.
10. National Center for Injury Prevention and Control Centers for Disease Control and Prevention. *Injury Fact Book of the Center for Disease Control and Prevention (CDC)*. Atlanta, GA: The National Center for Injury Prevention and Control; 2001:2001-2002.
11. Black JM, Edsberg LE, Baharestani MM, et al.; National Pressure Ulcer Advisory PanelPressure ulcers: avoidable or unavoidable? Results of the National Pressure Ulcer Advisory Panel Consensus Conference. *Ostomy Wound Manage*. 2011;57(2):24-37.
12. Halfens RJ, Bours GJ, Van Ast W. Relevance of the diagnosis 'stage 1 pressure ulcer': an empirical study of the clinical course of stage 1 ulcers in acute care and long-term care hospital populations. *J Clin Nurs*. 2001;10(6):748-757.
13. Gillespie BM, Chaboyer WP, McInnes E, Kent B, Whitty JA, Thalib L. Repositioning for pressure ulcer prevention in adults. *Cochrane Database Syst Rev*. 2014;3(4):CD009958.
14. Spruce L. Back to basics: preventing perioperative pressure injuries. *AORN J*. 2017;105(1):92-99.
15. Gefen A, Gershon S. An observational, prospective cohort pilot study to compare the use of subepidermal moisture measurements versus ultrasound and visual skin assessments for early detection of pressure injury. *Ostomy Wound Manage*. 2018;64(9):12-27.
16. Vangilder C, Macfarlane GD, Meyer S. Results of nine international pressure ulcer prevalence surveys: 1989 to 2005. *Ostomy Wound Manage*. 2008;54(2):40-54.
17. Gefen A, Farid KJ, Shaywitz I. A review of deep tissue injury development, detection and prevention: shear savvy. *Ostomy Wound Manage*. 2013;59(2):26-35.
18. Bates-Jensen BM, McCreath HE, Pongquan V, Apeles NC. Subepidermal moisture differentiates erythema and stage I pressure ulcers in nursing home residents. *Wound Repair Regen*. 2008;16 (2):189-197.
19. Bates-Jensen BM, McCreath HE, Pongquan V. Sub-epidermal moisture is associated with early pressure ulcer damage in nursing home residents with dark skin tones: pilot findings. *J Wound Ostomy Continence Nurs*. 2009;36(3):277-284.
20. Gefen A. The sub-epidermal moisture scanner: the principles of pressure injury prevention using novel early detection technology. *Wounds Int*. 2018;9(3):10-15.
21. Aoi N, Yoshimura K, Kadono T, et al. Ultrasound assessment of deep tissue injury in pressure ulcers: possible prediction of pressure ulcer progression. *Plast Reconstr Surg*. 2009;124(2):540-550.
22. Higashino T, Nakagami G, Kadono T, et al. Combination of thermographic and ultrasonographic assessments for early detection of deep tissue injury. *Int Wound J*. 2014;11(5):509-516.
23. Osman B, Kernodle MH. A new look at pressure ulcers: ultrasound technology can help detect skin integrity issues that are not apparent in a visual skin assessment. *Provider*. 2007;33(4): 35-37.
24. Scheiner J, Farid K, Raden M, Demisse S. Ultrasound to detect pressure-related deep tissue injuries in adults admitted via the emergency department: a prospective, descriptive, pilot study. *Ostomy Wound Manage*. 2017;63(3):36-46.
25. Yabunaka K, Iizaka S, Nakagami G, et al. Can ultrasonographic evaluation of subcutaneous fat predict pressure ulceration? *J Wound Care*. 2009;18(5):192, 194, 196.
26. Moore Z, Patton D, Rhodes SL, O'Connor T. Subepidermal moisture (SEM) and bioimpedance: a literature review of a novel method for early detection of pressure-induced tissue damage (pressure ulcers). *Int Wound J*. 2017;14(2):331-337.
27. Gefen A. The future of pressure ulcer prevention is here: detecting and targeting inflammation early. *EWMA J*. 2018;19(2):7-13.
28. Turner MD, Nedjai B, Hurst T, Pennington DJ. Cytokines and chemokines: at the crossroads of cell signalling and inflammatory disease. *Biochim Biophys Acta*. 2014;1843(11):2563-2582.
29. Clendenin M, Jaradeh K, Shamirian A, Rhodes SL. Inter-operator and inter-device agreement and reliability of the SEM Scanner. *J Tissue Viability*. 2015;24(1):17-23.
30. Gefen A. Managing inflammation by means of polymeric membrane dressings in pressure ulcer prevention. *Wounds Int*. 2018;9 (1):22-28.
31. Kim CG, Park S, Ko JW, Jo S. The relationship of subepidermal moisture and early stage pressure injury by visual skin assessment. *J Tissue Viability*. 2018;27(3):130-134.
32. Bates-Jensen BM, McCreath HE, Kono A, Apeles NCR, Alessi C. Sub-epidermal moisture predicts erythema and stage 1 pressure ulcers in nursing home residents: a pilot study. *J Am Geriatr Soc*. 2007;55(8):1199-1205.
33. Guihan M, Bates-Jenson BM, Chun S, Parachuri R, Chin AS, McCreath H. Assessing the feasibility of subepidermal moisture to predict erythema and stage 1 pressure ulcers in persons with spinal cord injury: a pilot study. *J Spinal Cord Med*. 2012;35(1):46-52.
34. Ching CT, Chou MY, Jiang SJ, et al. Tissue electrical properties monitoring for the prevention of pressure sore. *Prosthet Orthot Int*. 2011;35(4):386-394.
35. Harrow JJ, Mayrovitz HN. Subepidermal moisture surrounding pressure ulcers in persons with a spinal cord injury: a pilot study. *J Spinal Cord Med*. 2014;37(6):719-728.
36. Bates-Jensen BM, McCreath HE, Patlan A. Subepidermal moisture detection of pressure induced tissue damage on the trunk: the pressure ulcer detection (PUD) study outcomes. *Wound Repair Region*. 2017;25(3):502-511.
37. Bates-Jensen BM, McCreath HE, Nakagami G, Patlan A. Subepidermal moisture detection of heel pressure injury: the pressure ulcer detection (PUD) study outcomes. *Int Wound J*. 2018;15(2): 297-309.
38. Gershon S, Okonkwo H, Rhodes S, Burns M. SEM Scanner readings to assess pressure induced tissue damage. Paper presented at:

Proceedings of the 17th Annual European Pressure Ulcer Advisory Panel (EPUAP) Meeting; 2014; Sweden.
39. Bullough L. Chasing Zero pressure ulcer prevention and root cause analyses with the SEM Scanner. Paper presented at: 25th Conference of the European Wound Management Association; 2015; England.
40. Amlung SR, Miller WL, Bosley LM. The 1999 National Pressure Ulcer Prevalence Survey: a benchmarking approach. *Adv Skin Wound Care*. 2001;14(6):297-301.
41. Cheneworth CC, Hagglund KH, Valmassoi B, Brannon C. Portrait of practice: healing heel ulcers. *Adv Wound Care*. 1994;7(2): 44-48.
42. Fowler E, Scott-Williams S, McGuire JB. Practice recommendations for preventing heel pressure ulcers. *Ostomy Wound Manage*. 2008;54(10):42 –48, 50–52, 54–57.
43. Salcido R. What is the "purple heel"? *Adv Skin Wound Care*. 2006;19(1):11.
44. VanGilder C, MacFarlane GD, Harrison P, Lachenbruch C, Meyer S. The demographics of suspected deep tissue injury in the United States: an analysis of the international pressure ulcer prevalence survey 2006–2009. *Adv Skin Wound Care*. 2010;23(6): 254-261.
45. Sopher R, Nixon J, McGinnis E, Gefen A. The influence of foot posture, support stiffness, heel pad loading and tissue mechanical properties on biomechanical factors associated with a risk of heel ulceration. *J Mech Behav Biomed Mater*. 2011;4(4):572-582.
46. Gefen A. The biomechanics of heel ulcers. *J Tissue Viability*. 2010;19(4):124-131.
47. Levy A, Frank MB, Gefen A. The biomechanical efficacy of dressings in preventing heel ulcers. *J Tissue Viability*. 2015;24(1):1-11.
48. Hess DR. Noninvasive ventilation for acute respiratory failure. *Respir Care*. 2013;58(6):950-972.
49. Zhan Q, Sun B, Liang L, et al. Early use of noninvasive positive pressure ventilation for acute lung injury; a multicenter randomized controlled trial. *Crit Care Med*. 2012;40(2):455-460.
50. Munckton K, Ho KM, Dobb GJ, Das-Gupta M, Webb SA. The pressure effects of facemasks during noninvasive ventilation: a volunteer study. *Anaesthesia*. 2007;62(11):1126-1131.
51. Demoule A, Chevret S, Carlucci A; oVNI Study GroupREVA Network (Research Network in Mechanical Ventilation)Changing use of noninvasive ventilation in critically ill patients: trends over 15 years in francophone countries. *Intensive Care Med*. 2016;42 (1):82-92.
52. Black JM, Cuddigan JE, Walko MA, Didier LA, Lander MJ, Kelpe MR. Medical device related pressure ulcers in hospitalized patients. *Int Wound J*. 2010;7(5):358-365.
53. Worsley PR, Prudden G, Gower G, Bader DL. Investigating the effects of strap tension during non-invasive ventilation mask application: a combined biomechanical and biomarker approach. *Med Devices (Auckl)*. 2016;9:409-417.
54. Weng MH. The effect of protective treatment in reducing pressure ulcers for non-invasive ventilation patients. *Intensive Crit Care Nurs*. 2008;24(5):295-299.
55. Navalesi P, Fanfulla F, Frigerio P, Gregoretti C, Nava S. Physiologic evaluation of noninvasive mechanical ventilation delivered with three types of masks in patients with chronic hypercapnic respiratory failure. *Crit Care Med*. 2000;28(6):1785-1790.
56. Rozzini R, Sabatini T, Trabucchi M. Non-invasive ventilation for respiratory failure in elderly patients. *Age Ageing*. 2006;35(5): 546-547.
57. Tenenbaum S, Shabshin N, Levy A, Herman A, Gefen A. Effects of foot posture and heel padding devices on soft tissue deformations under the heel in supine position in males: MRI studies. *J Rehabil Res Dev*. 2013;50(8):1149-1156.
58. *Visible Human Project Gallery*. Bethesda MD: U.S. National Library of Medicine; 1994.
59. Friedman R, Haimy A, Gefen A, Epstein Y. Three-dimensional biomimetic head model as a platform for thermal testing of protective goggles for prevention of eye injuries. *Clin Biomech*. 2018. https://doi.org/10.1016/j.clinbiomech.2018.04.012
60. Mayrovitz HN. Assessing free and bound water in skin at 300 MHz using tissue dielectric constant measurements with the MoistureMeterD. In: Greene A, Slavin S, Brorson H, eds. *Lymphedema*. Cham, Switzerland: Springer International Publishing AG; 2015:133-148.
61. Schwan HP, Kay CF. Capacitive properties of body tissues. *Circ Res*. 1957;5:439-443.

How to cite this article: Peko Cohen L, Gefen A. Phantom testing of the sensitivity and precision of a sub-epidermal moisture scanner. *Int Wound J*. 2019; 16:979–988. https://doi.org/10.1111/iwj.13132